Escola de Primavera de Transição e Turbulência
Blumenau 2022

ABCM
13th Spring School on Transition and Turbulence
September 19th-23rd, 2022, Blumenau, SC, Brazil

EPTT-2022-0048
STUDY OF COMPRESSIBLE DIRECT NUMERICAL SIMULATIONS OF TOLLMIEN-SCHLICHTING WAVES INTERACTING WITH BUMPS

Ana Elisa Basilio de Carvalho[1]
Fernando H T Himeno[2]
Marlon Sproesser Mathias[3]
Marcello Augusto Faraco de Medeiros[4]
[1 2 4] São Carlos School of Engineering, University of São Paulo, EESC-USP.
[3] Institute of Advanced Studies, USP.
[1] anaelisabasilio@usp.br, [2] fernando.himeno@usp.br, [3] marlon.mathias@usp.br, [4] marcello@sc.usp.br

Abstract. *Through Direct Numerical Simulations (DNS), this work investigates the boundary layer stability of two-dimensional TS waves over a smooth plate with a two-dimensional isolated bump immersed in a compressible laminar boundary layer flow. The objective of the current work is to investigate aspects of the linear regime with the DNS code for hydrodynamic instability analysis on different Mach numbers. The numerical simulations were performed by a high order DNS for the compressible Navier-Stokes equations, developed by the Group of Aeroacoustics, Transition and Turbulence (GATT) of the Department of Aeronautical Engineering of the São Carlos School of Engineering, University of São Paulo (EESC-USP). A rectangular bump is positioned on a smooth plate. Five different bumps were defined by their height, proportional to the boundary layer displacement thickness at the position of the center of the bump on the smooth plate, that is, 0.05, 0.10, 0.20, 0.30 and 0.40. Upstream from the bump, there is a region capable of generating disturbances that travel downstream, interacting with the bump. For each height, a different base flow was generated, as well as for each Mach number on the subsonic and transonic regimes, 0.1, 0.3, 0.6, 0.7, 0.8 and 0.9. For each base flow, it was introduced a sinusoidal two-dimensional T-S wave with constant amplitude and frequency.*

Keywords: *bump, TS wave, Direct Numerical Simulation, boundary layer stability*

1. INTRODUCTION

In the aeronautical industry, structures similar to small bumps on a smooth surface, or an isolated roughness on a flat plate, are commonly present on aircraft surfaces, and can influence the drag coefficient if there is transition to the turbulent regime in the boundary layer. Even with a relatively small influence, preventing multiple sources like these is an interesting study that can be beneficial in saving fuel and operating costs.

The boundary layer transition is a process that can be initiated by instabilities. There is a large number of factors that influence on transition, several of which are interdependent. The study of each aspect individually promotes a better understanding of the complete mechanism and allows predictive modeling of phenomena, a great advantage in the aeronautical industry. In boundary layer flows, transition is often caused by primary instabilities and, as a consequence, the amplification of secondary instabilities. For small Mach numbers, the main primary instability source of these flows is the two-dimensional TS wave.

Through Direct Numerical Simulations (DNS), the objective of the current work is to investigate the effects of two-dimensional TS waves over a flat plate with a two-dimensional isolated roughness element immersed in a compressible laminar boundary layer flow.

2. REVIEW

Early works investigated roughness elements and isolated imperfections on the surface of airfoils with zero pressure gradient or flat plates as factors that promoted transition from laminar to turbulent flow. Wind tunnel experiments from Fage (1943), Tani (1961, 1969) and those shown in the review by Dryden (1953) indicated that a smoother surface influenced in the conservation of stability in a laminar boundary layer. Therefore, to conserve laminar flow it was of great importance to establish the highest height h of the structures that could be tolerated without influencing the transition. For some combinations of roughness height-thickness ratio dependent, stream speed and location of roughness element, it was also determined that, for higher flow speeds, the distance between roughness and the transition point was gradually reduced.

On studies about two-dimensional roughnesses with disturbances, such as Klebanoff and Tidstrom (1972), Dovgal and Kozlov (1990), Morkovin (1990) and Wörner *et al.* (2003), it was concluded that the flow region modified by the presence of the roughness is more sensitive to destabilizing influences. The degree of instability was dependent on the velocity profile and its interaction with the roughness geometry. The presence of waves with small oscillation amplitudes in the roughness region, around 1% of the velocity on the outer edge of the boundary layer U_0, already proved strong influence

on transition.

In stability theory for compressible flows, the primary interest is in unstable rather than neutral waves (Mack, 1987). The maximum spatial amplification rate as a function of Mach for 2D waves indicates that the second and higher modes are most unstable as 2D waves, because they depend on the thickness of the relative supersonic region, but the first mode is most unstable as an oblique wave at all supersonic Mach numbers. For lower Mach numbers, an oblique wave can have an amplification rate several times larger than a 2D wave. For $M < 2.4$, an oblique first-mode wave is even more unstable than a 2D second-mode wave. For Dunn and Lin (1955) as the Mach Number increases, three-dimensional disturbances become significant under conditions that are less and less extreme, until finally, at a Mach Number between one and two, they begin to play the leading role in many cases of practical interest.

Results in Lees (1947) and Lees and Reshotko (1962) indicate that, for the laminar boundary layer flow, the minimum critical Reynolds number decreases from its Mach number zero value, reaches a minimum somewhere around $M = 3$ and then increases again. In Criminale *et al.* (2018), it is shown that up to $M = 1.6$, the neutral stability curve is quite similar to the incompressible case, but at higher values of the Mach number the upper branch turns upward toward the inviscid limit. As pointed out by Mack in his calculations, inviscid disturbances begin to dominate at $M = 3$ and the stability characteristics are more like those of a free shear layer than of a low-speed zero-pressure gradient boundary layer.

3. METHODOLOGY

The numerical simulations were performed by a DNS for the compressible Navier-Stokes equations, developed by the Group of Aeroacoustics, Transition and Turbulence (GATT) of the Department of Aeronautical Engineering of the São Carlos School of Engineering, University of São Paulo (EESC-USP). The main works that present the development and validation of the DNS can be found in Bergamo (2014), Gaviria Martínez (2016), Mathias (2017), Mathias and Medeiros (2019).

In this work, the fourth order Runge-Kutta method is used for time marching. For the spatial derivatives, a sixth order compact spectral-like finite differences shown by Lele (1992) is used. The pre processing is done in MATLAB and the main processing is written in FORTRAN.

The governing equations were defined in a two-dimensional domain (x, y), and time (t), in terms of density (ρ), the two velocity components (u, v), and internal energy (e). The values presented here are non-dimensional, by the characteristic velocity at the outer edge of the boundary layer (U_0), the boundary layer displacement thickness at the roughness position (δ^*_R) and initial density (ρ_0).

For the boundary conditions, the inflow boundary is defined as an uniform flow at constant temperature and the pressure derivative is zero. In the outflow, pressure is kept constant and the second derivative is null for the other variables. The outer flow condition on the wall-normal direction sets the second derivative of all variables to zero.

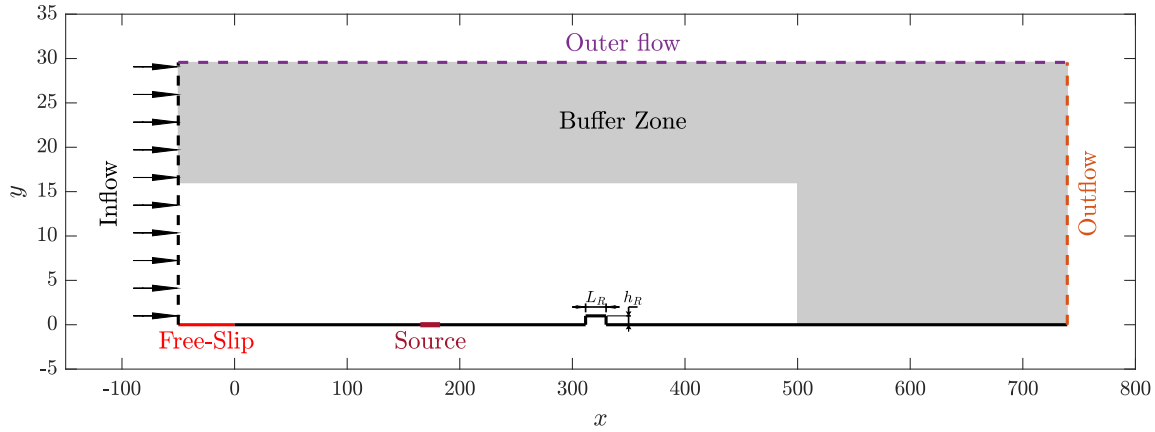

Figure 1. Illustration of the domain (non-dimensional)

For the walls, including the roughness, there are no-slip and no-penetration conditions for velocity, the pressure gradient is zero in the normal direction and the temperature is fixed. From $x = -50$ to $x = 0$ there is a free-slip region in the wall, necessary to accommodate the flow before the boundary layer starts forming.

A rectangular roughness placed on a flat plate, according to Fig. 1. Upstream from the roughness, there is a region capable of generating disturbances that travel downstream, interacting with the roughness.

Some flow parameters were taken from the experimental works by de Paula (2007) and de Paula *et al.* (2017), such as: Reynolds number in the position of the wave source $Re_{\delta^*_{TS}} = 700$, Reynolds number at the roughness position $Re_{\delta^*_R} = U_\infty \delta_{1,R}/\nu = 950$, roughness diameter $d = 10\ mm$ and displacement thickness at the experimental roughness location $\delta^*_R = 0.55\ mm$.

Five different bumps were defined by their height, proportional to the boundary layer displacement thickness at the position of the center of the bump on the smooth plate, that is, $\delta^*_R = 0.05, 0.10, 0.20, 0.30$ and 0.40. The initial condition is a Blasius boundary layer at constant temperature and pressure. The characteristic Reynolds number is $Re = 950$.

The meshes are Cartesian and initially uniform, which can be stretched in certain regions, increasing the density of nodes as needed, as seen on Fig. 2 and 3. For the flows with the roughness element, the mesh is refined in the x direction around the roughness region. In the y direction it is refined on the boundary layer region, and extra refined around the height of the roughness.

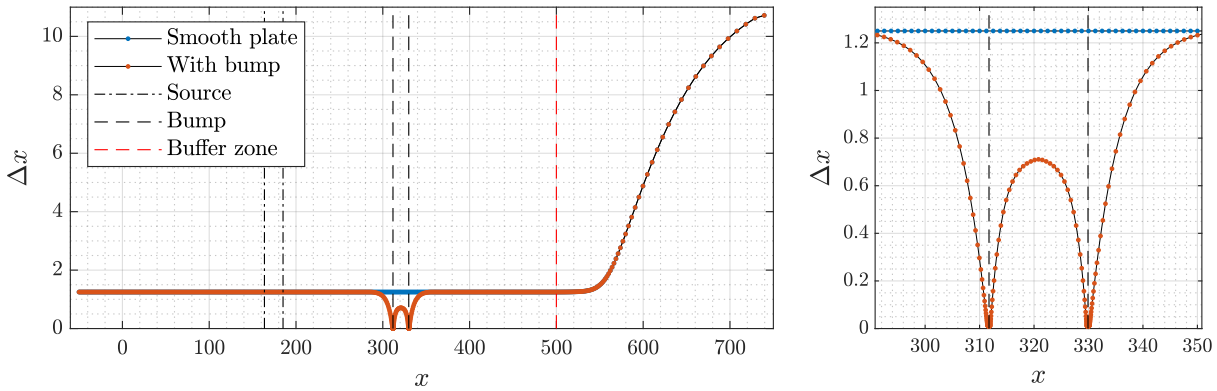

Figure 2. Mesh spacing (stream-wise direction)

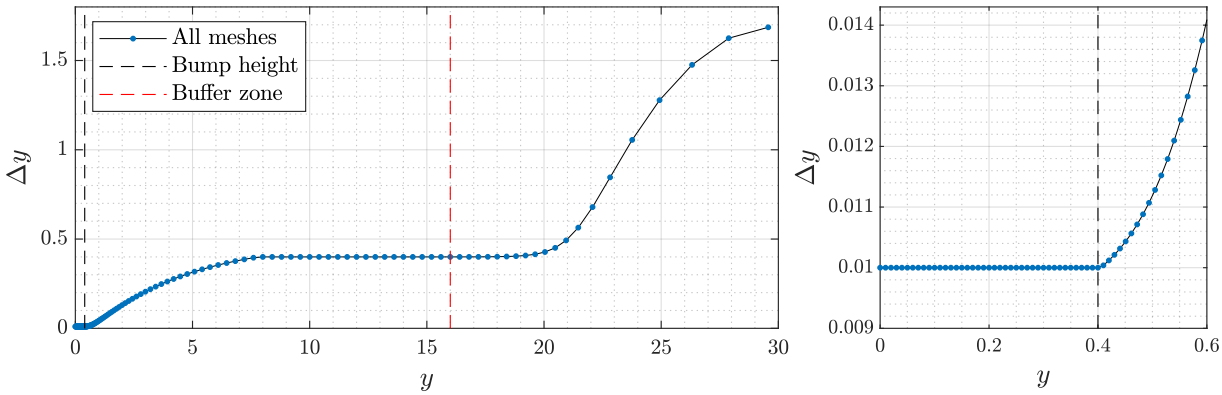

Figure 3. Mesh spacing (wall-normal direction)

The buffer zone consists of the region from $x = 500$ to the end of the mesh, which is included to avoid problems in the simulation, such as reflections in the domain. In y, there is a region with an intense refinement along the height of the roughness, from $y = 0$ to $y = 0.4$. The buffer zone starts at $y = 16$ and ends at the last node.

4. RESULTS

The results will be presented for $M = 0.1, 0.3, 0.6, 0.7, 0.8$ and 0.9. For each Mach number, a different base flow was generated for the flat plate and for the each plate with an isolated roughness, for comparison. Then, for all the base flows, it was introduced a sinusoidal two-dimensional TS with constant amplitude and frequency.

4.1 Base Flow

The simulation of flat plate with roughness has a maximum relative error close to the order of 10^{-12}, an adequate value for a base flow simulation for the following analysis. Using the equations in Schlichting and Gersten (2017), the displacement and momentum thickness of the boundary layer, δ^* and θ, respectively, were calculated and are shown in Fig. 4 and 5.

The roughness effects are proven to be mostly local, deforming the boundary layer both downstream and upstream, but seem to expand downstream from the element as the Mach number grows. For higher M, these values do not return to the flat plate values within the physical domain. It seems that the roughness height effects remain similar as the M changes. The distortion is also greater in value for θ as the Mach number grows, the opposite of what is shown for δ^*. The

curve format changes noticeably specially for θ from the increasing M, and as from $M = 0.8$, the height also contributes to this.

As the Mach number increases, as well as bump height, the boundary layer parameters take longer longitudinal distances to return to flat plate values. In some cases, particularly for every height at $M = 0.9$, it does not happen within the bounds of the regular domain, $x = 500$.

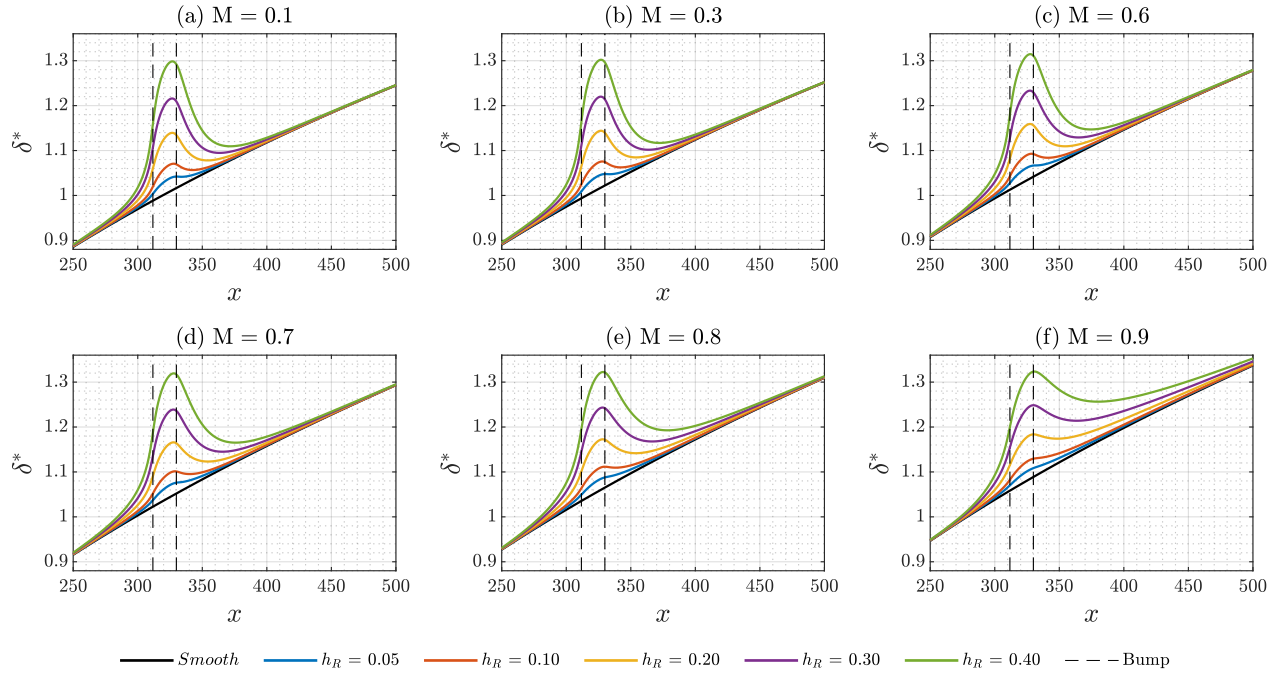

Figure 4. Base flow displacement thickness

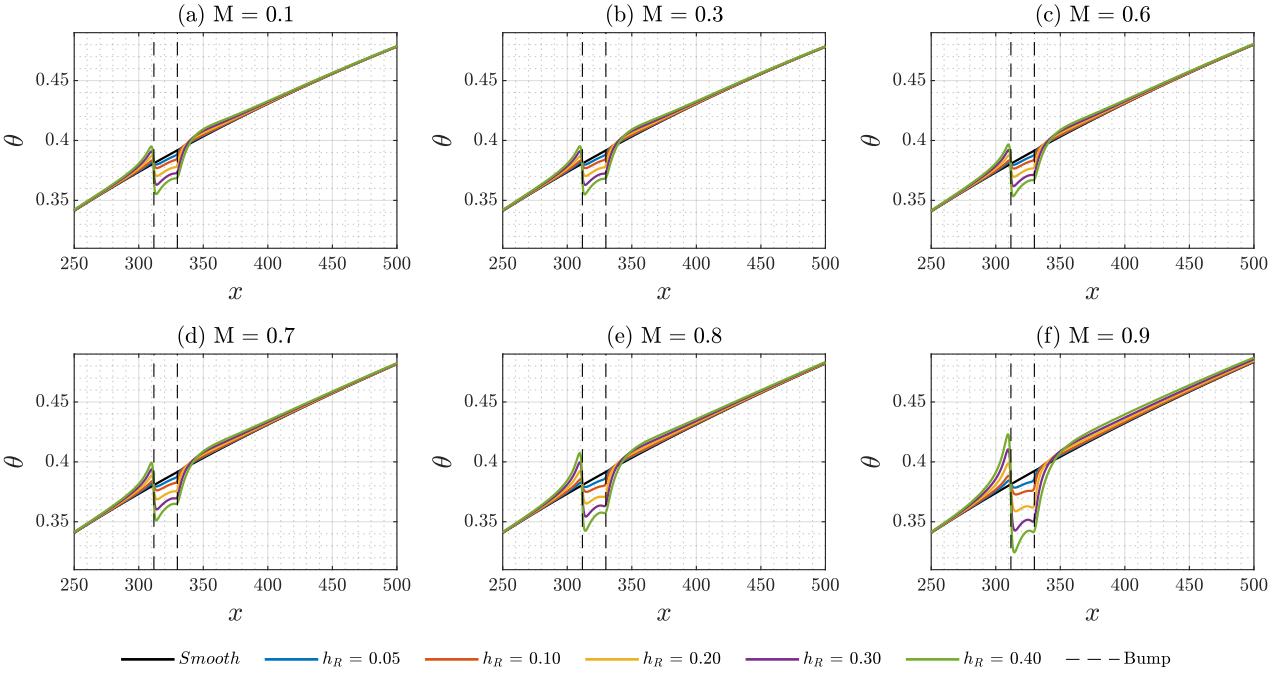

Figure 5. Base flow momentum thickness

4.2 Disturbed Flow

A sinusoidal two-dimensional TS wave was generated at the source with an amplitude within the linear regime and non-dimensional frequency $F = 90 \times 10^{-6}$, defined as shown in Fig. 6. The amplitude at the wave source had different values for each Mach number, with the intent of keeping the simulations within the linear regime.

This TS wave is a monochromatic excitation disturbance of the wall velocity u, periodic in both time and x, covering the most unstable band downstream from $Re_{\delta^*} = 950$.

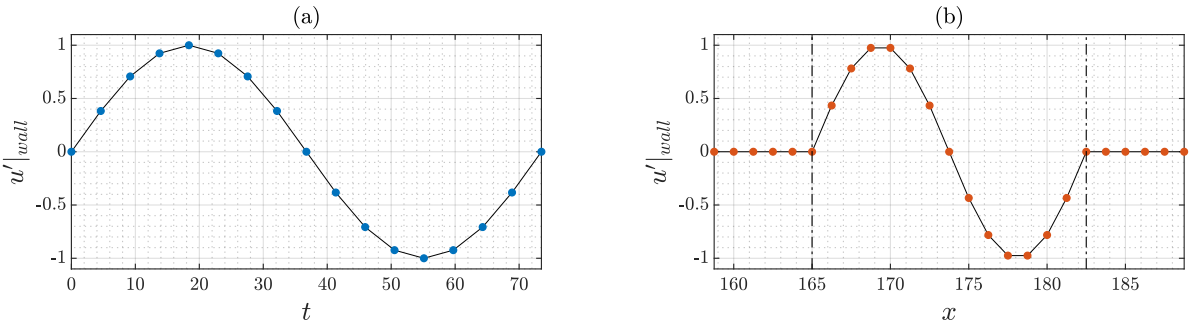

Figure 6. Monochromatic TS wave signal at the wall

4.2.1 The Effect of the Bump Height

Figure 7 shows the amplitude change caused by bumps of different heights. The amplification factor relative to the smooth surface is also shown for better visualization. The Mach number is $M = 0.1$ and the TS frequency is $F = 90 \times 10^{-6}$.

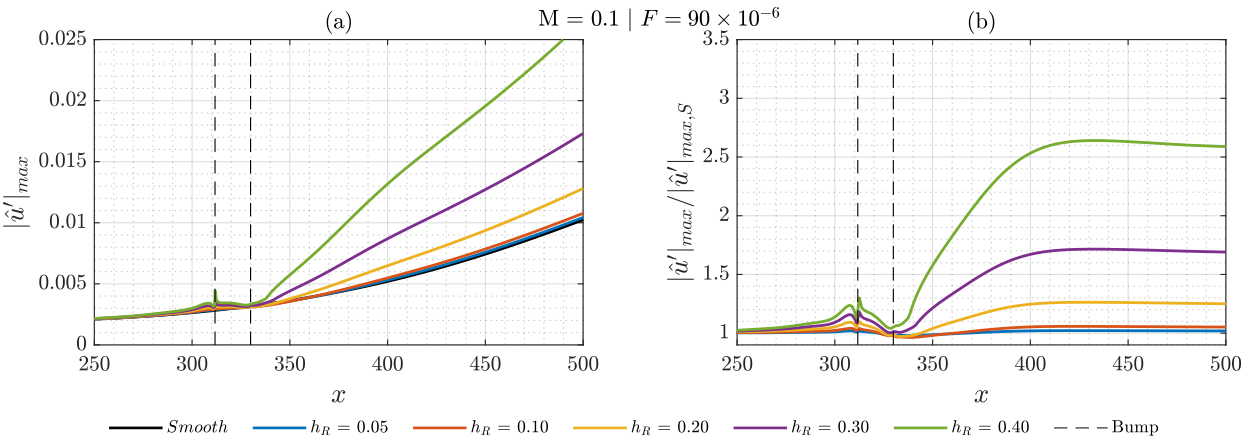

Figure 7. Amplitude evolution of the TS mode for different bump heights at $M = 0.1$

The TS amplitude increases with the bump height, as it was already shown by Wörner *et al.* (2003). For smaller bumps, up to $h_R = 0.1$, the amplitude change is relatively small, being very similar to the smooth plate case.

As the amplitude change varies considerably with height, it would be better to understand the problem with another approach rather than comparing the amplitude. For another perspective, the growth rates of these curves are plotted on Fig. 8. Calling the maximum absolute amplitude $|\hat{u}'|_{max}$ of simply A, the growth rate of this variable would be given as $GR = (dA/dx)/x$.

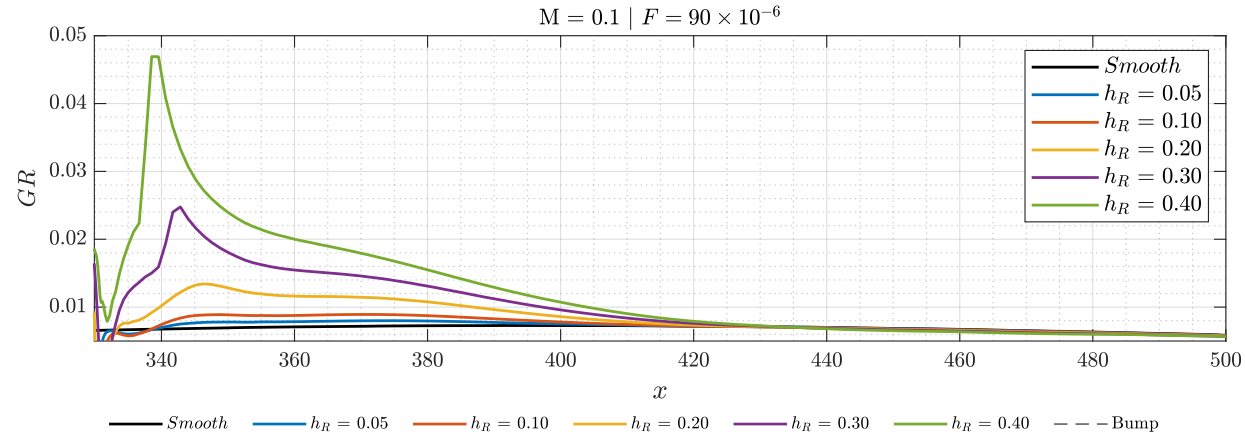

Figure 8. Growth rate change caused by bumps with different heights compared to the smooth plate at $M = 0.1$

The growth rate reaches a maximum over the plate even if no bump is present and then decays. The bump inclusion affects the growth rate locally and its maximum magnitude depends on height, but downstream the growth rate returns to that observed in the smooth plate. Moreover, the plate location where it occurs seems to be the same regardless of height. Thus, the region where growth rate differs from that of the smooth plate can be associated as the region of influence of each bump itself.

4.2.2 The Effect of Mach

The same analysis from previous section is now extended by comparing the results of low Mach regime, $M = 0.1$, to that obtained for $0.3, 0.6, 0.7, 0.8$ and 0.9. The effect of bump height change at these Mach numbers are shown in Fig. 9 comparing the smooth case to each bump height.

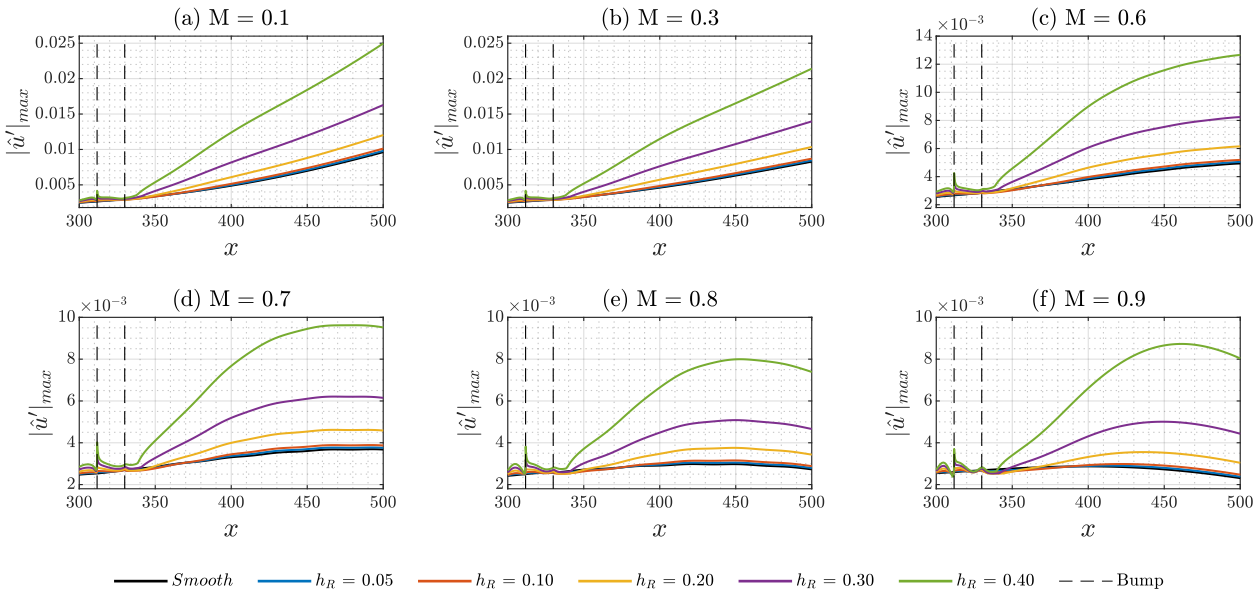

Figure 9. Amplitude evolution of the TS wave

For heights up to $h_R = 0.10$ the amplitude change is still small, with their evolution mainly following that of the smooth plate. For higher h_R, the amplitude change is quite different from the smooth one. In this scenario, as the Mach grows, the maximum amplitude values become smaller, indicating that the mode associated with this frequency becomes more stable. As the height also increases, the amplification in comparison with the smooth plate also grows, specially for the transonic cases.

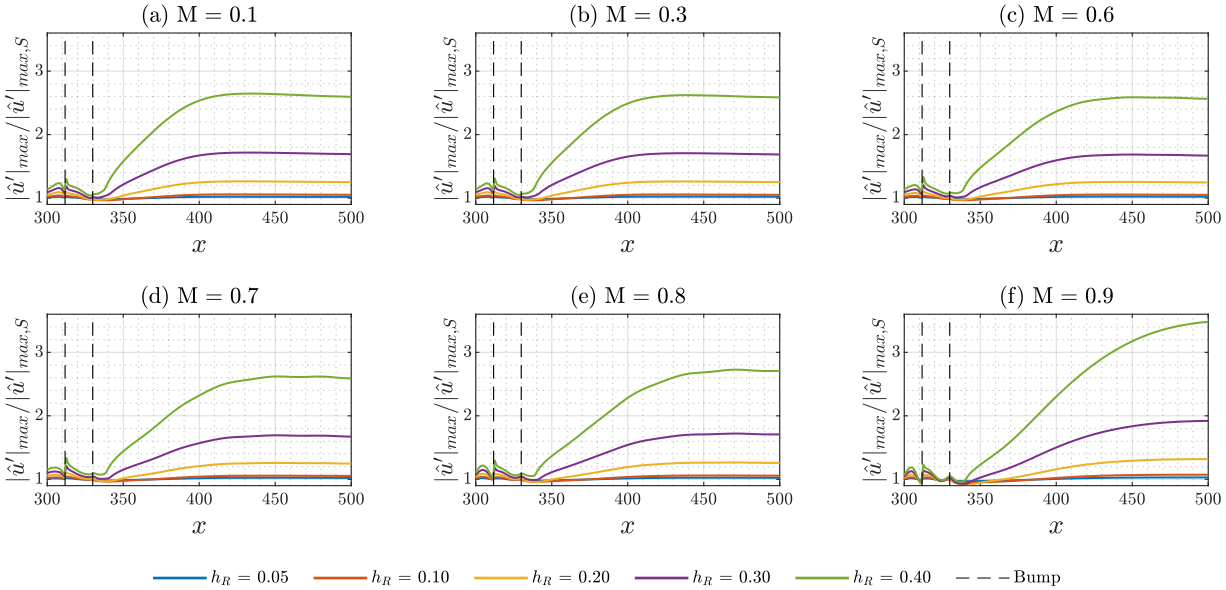

Figure 10. Amplitude evolution of the TS wave, normalized by the smooth plate amplitude

In Fig. 10 the amplitude factor relative the smooth plate is also plotted grouping all bump heights. At the subsonic regime, the amplitude factors are very similar, slightly decreasing with increasing Mach. But at transonic speeds, the opposite effect seems to occur, and the amplitude factors dramatically increase, specially at $M = 0.9$.

The growth rate is also investigated and results are presented in Fig. 11. It shows the region of bump influence has only small changes caused by compressible effects for subsonic regime, but for the transonic cases this influence region becomes much longer.

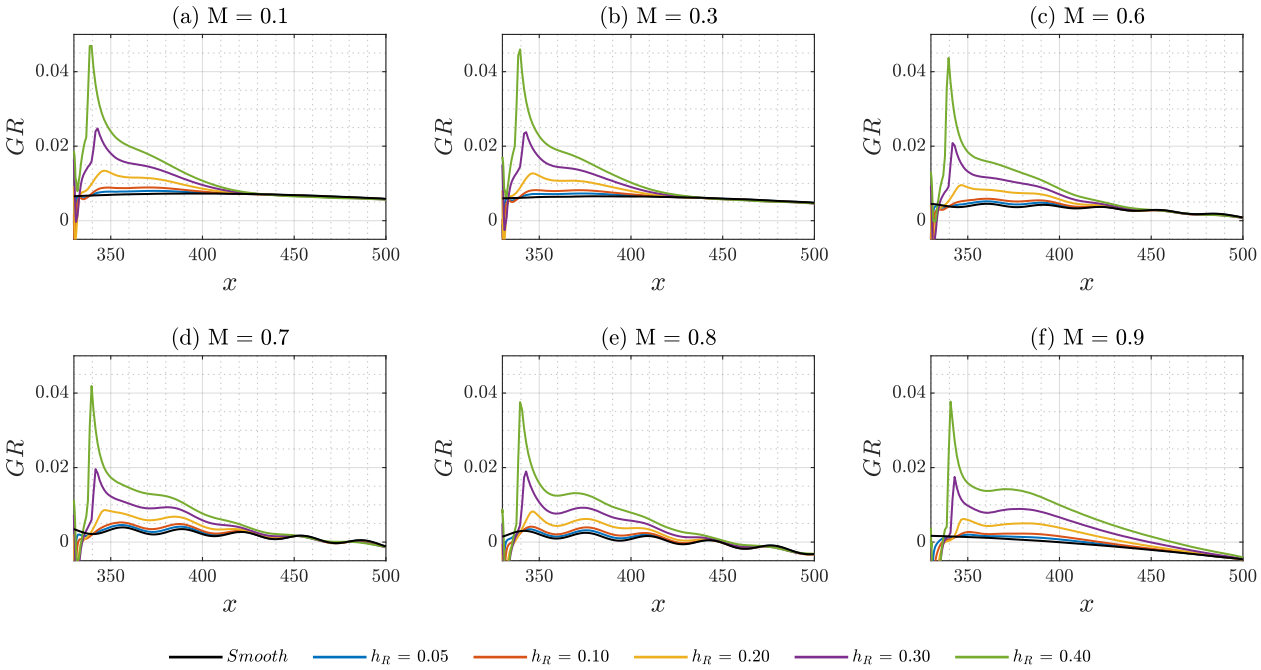

Figure 11. Growth rate change caused by bumps with different heights compared to the smooth plate

Since the chosen velocity component for the source disturbance is u, for it is a dipole wave with less acoustic emissions, it exhibits results with smaller oscillations. Despite that, some oscillations are present for $M = 0.6, 0.7$ and 0.8. This indicates a peculiarity around the beginning of the transonic range.

5. CONCLUSIONS

Through Direct Numerical Simulations, this work investigates the boundary layer stability of a sinusoidal two-dimensional Tollmien-Schlichting waves over a flat plate and plates with a two-dimensional isolated roughness element, immersed in a compressible laminar boundary layer flow.

The influence of Mach number on the effect of a bump on the TS wave evolution has not been yet addressed systematically. Here, it was found that for bump heights below 10%, the effect was comparatively negligible. Above it, the effect of the bump increased with both Mach, being more extensive in the stream-wise direction downstream from the bump, and with height, promoting greater amplification factors for taller bumps.

However, the effect at the roughness location itself is relatively small. The Mach effect is mostly a consequence of the downstream region affected by the bump, which increases substantially, in particular when approaching the supersonic regime.

6. ACKNOWLEDGEMENTS

This study was financed in part by the Coordenação de Aperfeiçoamento de Pessoal de Nível Superior - Brasil (CAPES) - Finance Code 001 and by São Paulo Research Foundation (FAPESP/Brazil) - project grant 2019/15336-7.

Research carried out using the computational resources of the Center for Mathematical Sciences Applied to Industry (CeMEAI) funded by FAPESP (grant 2013/07375-0).

F.H.T.H is sponsored by São Paulo Research Foundation (FAPESP/Brazil) grant #2018/02542-9.

M.S.M. is sponsored by São Paulo Research Foundation (FAPESP/Brazil) grant #2018/04584-0.

M.A.F.M. is sponsored by National Council for Scientific and Technological Development (CNPq/Brazil), grant #307956/2019-9.

We would like to thank the US Air Force Office of Scientific Research (AFOSR), grant FA9550-18-1-0112, managed by Dr. Geoff Andersen from SOARD (Southern Office of Aerospace Research and Development).

7. REFERENCES

Bergamo, L.F., 2014. *Instabilidade hidrodinâmica linear do escoamento compressível em uma cavidade*. Master's thesis.

Criminale, W.O., Jackson, T.L. and Joslin, R.D., 2018. *Theory and Computation in Hydrodynamic Stability*. Cambridge University Press.

de Paula, I.B., Würz, W., Mendonça, M.T. and Medeiros, M.A.F., 2017. "*Interaction of instability waves and a three-dimensional roughness element in a boundary layer*". Journal of Fluid Mechanics, Vol. 824, pp. 624–660.

de Paula, I.B., 2007. *Influência de uma rugosidade tridimensional isolada na transição de uma camada limite sem gradiente de pressão*. Ph.D. thesis, Universidade de São Paulo.

Dovgal, A.V. and Kozlov, V.V., 1990. "*Hydrodynamic Instability and Receptivity of Small Scale Separation Regions*". Laminar-Turbulent Transition, pp. 523–531.

Dryden, H.L., 1953. "*Review of Published Data on the Effect of Roughness on Transition from Laminar to Turbulent Flow*". Journal of the Aeronautical Sciences, pp. 447–482.

Dunn, D.W. and Lin, C.C., 1955. "*On the stability of the laminar boundary layer in a compressible fluid*". Journal of the Aeronautical Sciences, Vol. 22, pp. 455–477.

Fage, A., 1943. "*The smallest size of spanwise surface corrugation which affects boundary-layer transition on an airfoil*". Aeronautical Research Council, R & M 2120.

Gaviria Martínez, G.A., 2016. *Towards natural transition in compressible boundary layers*. Ph.D. thesis, Universidade de São Paulo.

Klebanoff, P.S. and Tidstrom, K.D., 1972. "*Mechanism by Which a Two-Dimensional Roughness Element Induces Boundary-Layer Transition*". The Physics of Fluids, Vol. 15, No. 7, pp. 1173–1188.

Lees, L., 1947. "*The stability of the laminar boundary layer in a compressible fluid*". NACA TR-876.

Lees, L. and Reshotko, E., 1962. "*Stability of the compressible laminar boundary layer*". Journal of Fluid Mechanics, Vol. 12, p. 555–590.

Lele, S.K., 1992. "*Compact Finite Difference Schemes with Spectral-like Resolution*". Journal of Computational Physics, Vol. 106, pp. 16–42.

Mack, L., 1987. "*Review of compressible stability theory*". In *Stability of time dependent and spatially varying flows*. Springer.

Mathias, M.S., 2017. *Instability analysis of compressible flows over open cavities by a Jacobian-free numerical method*. Master's thesis, Universidade de São Paulo.

Mathias, M.S. and Medeiros, M.F., 2019. *Global instability analysis of a boundary layer flow over a small cavity*.

Morkovin, M.V., 1990. "*On Roughness-Induced Transition: Facts, Views, and Speculations*". pp. 281–295.

Schlichting, H. and Gersten, K., 2017. *Boundary-Layer Theory*. Springer, Berlin, Heidelberg.

Tani, I., 1961. "*Effect of Two-Dimensional and Isolated Roughness on Laminar Flow*". Boundary Layer and Flow Control, Vol. 2, pp. 637–656.

Tani, I., 1969. "*Boundary Layer Transition*". Annual Review of Fluid Mechanics, Vol. 1, pp. 169–196.

Wörner, A., Rist, U. and Wagner, S., 2003. "*Humps/Steps Influence on Stability Characteristics of Two-Dimensional Laminar Boundary Layer*". AIAA Journal, Vol. 41, No. 2, pp. 192–197.

8. RESPONSIBILITY NOTICE

The authors are the only responsible for the printed material included in this paper.